Seismic Monitoring of the North Korea Nuclear Test Site Using a Multichannel Correlation Detector

Steven J. Gibbons, *Member, IEEE*, and Frode Ringdal

***Abstract*—North Korea announced a second nuclear test on 25 May 2009, the first having taken place on October 9, 2006. Both tests were detected by the global seismic network of the Comprehensive nuclear Test-Ban-Treaty Organisation. We apply a correlation detector using a 10-s signal template from the 2006 test on the MJAR array in Japan to: 1) assess the potential for automatically detecting subsequent explosions at or near the test site; and 2) monitor the associated false alarm rate. The 2009 signal is detected clearly with no false alarms in a three-year period. By detecting scaled-down copies of the explosion signals submerged into background noise, we argue that a significantly smaller explosion at the site would have been detected automatically, with a low false alarm rate. The performance of the correlator on MJAR is not diminished by the signal incoherence that makes conventional array processing problematic at this array. We demonstrate that false alarm elimination by f-k analysis of single channel detection statistic traces is crucial for maintaining a low detection threshold. Correlation detectors are to be advocated as a routine complement to the existing pipeline detectors, both for reducing the detection threshold for sites of interest and providing automatic classification of signals from repeating sources.**

***Index Terms*—Array signal processing, arrays, correlation, detectors, matched filters, nuclear explosions, seismic waves, seismology.**

I. Introduction

On October 9, 2006, the Democratic People's Republic of Korea (DPRK or North Korea) announced that an underground nuclear test had been carried out, a claim which was rapidly supported by recordings on seismic sensors at distances of up to many thousands of kilometers. This test, carried out by a nonsignatory state to the Comprehensive nuclear Test-Ban-Treaty (CTBT), provided a very useful test of the regime for verification of compliance with the treaty. The International Monitoring System (IMS) consists of a global network of seismic, infrasonic, hydroacoustic, and radionuclide sensors deployed to detect and identify events which could constitute a violation of the treaty, and the data generated are transmitted in near real-time for processing at the International Data Center (IDC) in Vienna (see [1]). In terms of event detection and location, the IMS and IDC passed the test convincingly. Signals from this relatively low yield explosion were detected and classified correctly by many primary seismic IMS stations at teleseismic distances and a high quality, fully automatic, event location estimate resulted. Magnitude estimates of 4.1 and 4.2, respectively, were reported by the IDC and the U.S. Geological Survey.

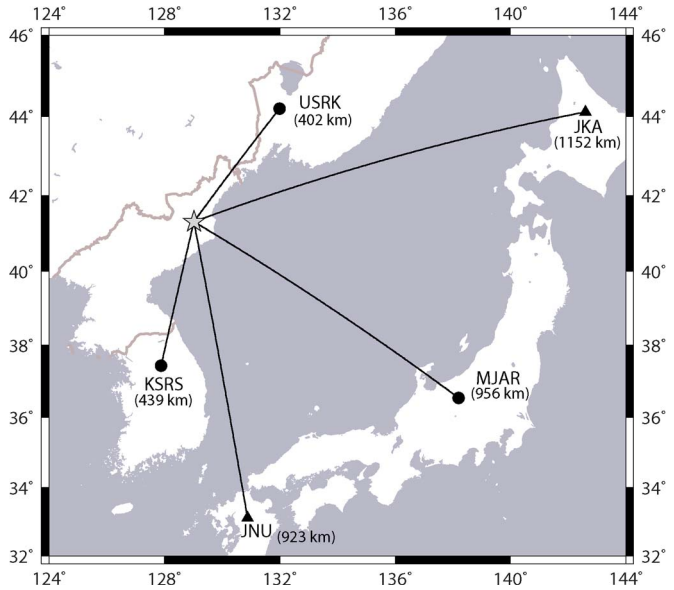

Fig. 1. Location estimate for the May 25, 2009, North Korea nuclear test with respect to the closest five IMS stations. Circles indicate primary seismic array stations and triangles indicate auxilliary three-component stations.

This test was the first of its kind since the IDC became operational in February 2000. The seismic signals generated have been examined extensively to address fundamental questions regarding the effectiveness of the verification regime; down to what magnitude can the IMS confidently detect and locate a seismic event in a target source region [2], and to what extent can the signals allow discrimination between an explosion and an earthquake [3], [4]. On May 25, 2009, a second test was carried out. This significantly larger event was readily detected and automatically located by a far more complete IMS network, now including three primary seismic arrays within 1000 km (Fig. 1). The source parameters of the two nuclear tests as estimated by the IDC, based upon measurements on IMS stations, are given in Table I. The analyst reviewed location estimates for the two events are in close proximity. Significantly, however, waveforms at various stations from the two explosions were similar enough to allow for high precision measurements of relative arrival times from which very accurate relative location estimates can be obtained (see [5] and [6]). Two independent studies using regional [7] and teleseismic [8] arrivals placed the 2009 test approximately 2 km to the west and slightly to the north of the 2006 test.

Manuscript received February 25, 2011; revised August 3, 2011; accepted September 25, 2011. Date of publication October 28, 2011; date of current version April 18, 2012.

The authors are with NORSAR, 2027 Kjeller, Norway (e-mail: steven@norsar.no; frode@norsar.no).

Color versions of one or more of the figures in this paper are available online at http://ieeexplore.ieee.org.

Digital Object Identifier 10.1109/TGRS.2011.2170429

0196-2892/$26.00 © 2011 IEEE

TABLE I
LOCATION AND ORIGIN TIME ESTIMATES FROM THE REVIEWED EVENT BULLETIN (REB) OF THE IDC FOR THE DPRK NUCLEAR TESTS ON 9 OCTOBER 2006 AND 25 MAY 2009

Origin time	Latitude	Longitude	m_{b} estimate
2006-282:01.35.27.58	41.3119	129.0189	4.1
2009-145:00.54.42.80	41.4110	129.0464	4.5

Of the three primary seismic arrays in Fig. 1, only MJAR (Matsushiro, Japan) was certified at the time of the 2006 test. For both events, despite high signal-to-noise ratio (SNR) arrivals, MJAR failed to generate a detection with qualitatively correct parameter estimates at the time of the first signal arrival, and so failed to contribute to the automatic preliminary event location estimates. Array processing at this station is notoriously difficult due to signal incoherence between the sensors. This has been documented for teleseismic signals [9] which are typically rich in low frequency energy, and the problems are likely to be exacerbated for the higher frequencies and increased scattering anticipated for signals from events at regional distances (< 2000 km). It was demonstrated [10] that incoherent direction estimates, made possible by the relatively large time delays between sensors, were more stable than estimates using classical array processing (e.g., [11]).

The KSRS array (a legacy array in South Korea, originally named KSAR, see, e.g., [12]) did record the 2006 test but, prior to certification, this data was not available to the IDC. KSRS was certified on October 31, 2006, and the new USRK array in the Russian Federation provided data for the first time in 2008. A study of IMS detectability for the North Korea test site [2] concluded that the KSRS array was crucial for maintaining a threshold monitoring capability below magnitude 3. The demonstrated similarity between the signals from the two tests makes this monitoring scenario an ideal candidate for monitoring using a correlation or matched filter detector which exploits the existing signal to detect occurrences of similar signals from subsequent colocated or very nearby events. Significantly, when correlating over seismic arrays or networks, no semblance is required between the waveforms on different sensors [13] meaning that the characteristics of the MJAR recordings are no hindrance.

The purpose of this paper is to explore the extent to which the North Korea test site can be monitored seismically using correlation techniques, with emphasis on MJAR. It is almost a corollary of the waveform similarity exploited for the relative location estimates [7], [8] that the signal from the second test can be detected using a template comprising the signal from the first test. However, the false alarm rate associated with such a procedure needs to be determined (is the number of false positives low enough for the procedure to be worthwhile?) as does the likely detection rate for lower amplitude signals from smaller yield tests at the site.

II. SEISMIC OBSERVATIONS ON IMS ARRAYS AT REGIONAL DISTANCES

The differences in the regional waveforms as a function of backazimuth from the test site have been discussed and interpreted in terms of the structure along the various propagation paths [14]. By the time of the 2009 test, paths of almost equal distance at two very different backazimuths were covered by the certified primary IMS seismic arrays KSRS and USRK (Fig. 2). The SNR at a given station, for a signal generated by an event in a particular source region, is a useful parameter in estimating the anticipated detection threshold for subsequent events in that source region (see, for example, [15] and [16]). The initial P arrivals generated by the 2009 DPRK nuclear test are associated with a high SNR at both the KSRS and USRK arrays, indicating a significant improvement in the detection capability for the test site for the more complete IMS.

Seismic arrays estimate the apparent velocity and backazimuth of incoming wavefronts (phases) by delaying and stacking waveforms from neighboring sites (i.e., variations of beamforming, e.g., [18] and [19]). The backazimuth (the direction from which the wavefront approaches the array) is an important parameter in the phase association and event location procedure, and the apparent velocity is often crucial for phase identification. At regional distances, Pn and Pg (see [20] for definitions) are P-waves which travel through the (faster) uppermost mantle and (slower) crust, respectively. Pn usually approaches a station with a steeper angle of incidence than Pg, resulting in a higher apparent velocity. The correct identification of these phases, together with good estimates of the time separating them, may be crucial for estimating the epicentral distance. Sn and Sg are S-waves which follow the same paths as Pn and Pg, respectively, and Lg denotes a packet of S-wave energy trapped in the crust [21].

Arrays almost always have an advantage over three-component stations for parameter estimation in that no model of the particle motion is required and that high quality estimates can also be obtained for secondary phases (e.g., [22]). The limitations are almost invariably caused by a degradation of signal coherence between sensors (see [23]). In the VESPA process [17], the morphology of the wavefield evolving over an array can be visualized by displaying the coherent energy content over a range of slowness vectors (directions of arrival) as a function of time. Fig. 2 indicates that Pn and the later arriving Pg are visible at both arrays. At USRK, Pg (characterized by a lower apparent velocity) is significantly stronger than Pn; at KSRS, it is significantly weaker. At USRK, the Sn phase is not observed above the strong P-coda, whereas a clear Lg phase is observed over a minute after the initial P-arrival. At KSRS, Sn is clearly visible on the vespagram whereas no distinct Lg phase onset can be identified.

The sharper definition of the peaks in the lower panel of Fig. 2 is a result of the greater array aperture of KSRS (see Fig. 3). At a given frequency, a wider array aperture will provide a higher resolution of slowness space, provided that the signals on the different sensors remain sufficiently coherent. While P-arrivals are typically more coherent to higher frequencies than the more scattered secondary phases (e.g., [24]), it can be demonstrated the 2–4 Hz frequency band used for the analysis in Fig. 2 pushes coherent processing to the limit at both arrays for all phases. f-k analysis at higher frequencies would be desirable due to the significant high-frequency content of the signals and the theoretical improvement to the resolution in slowness

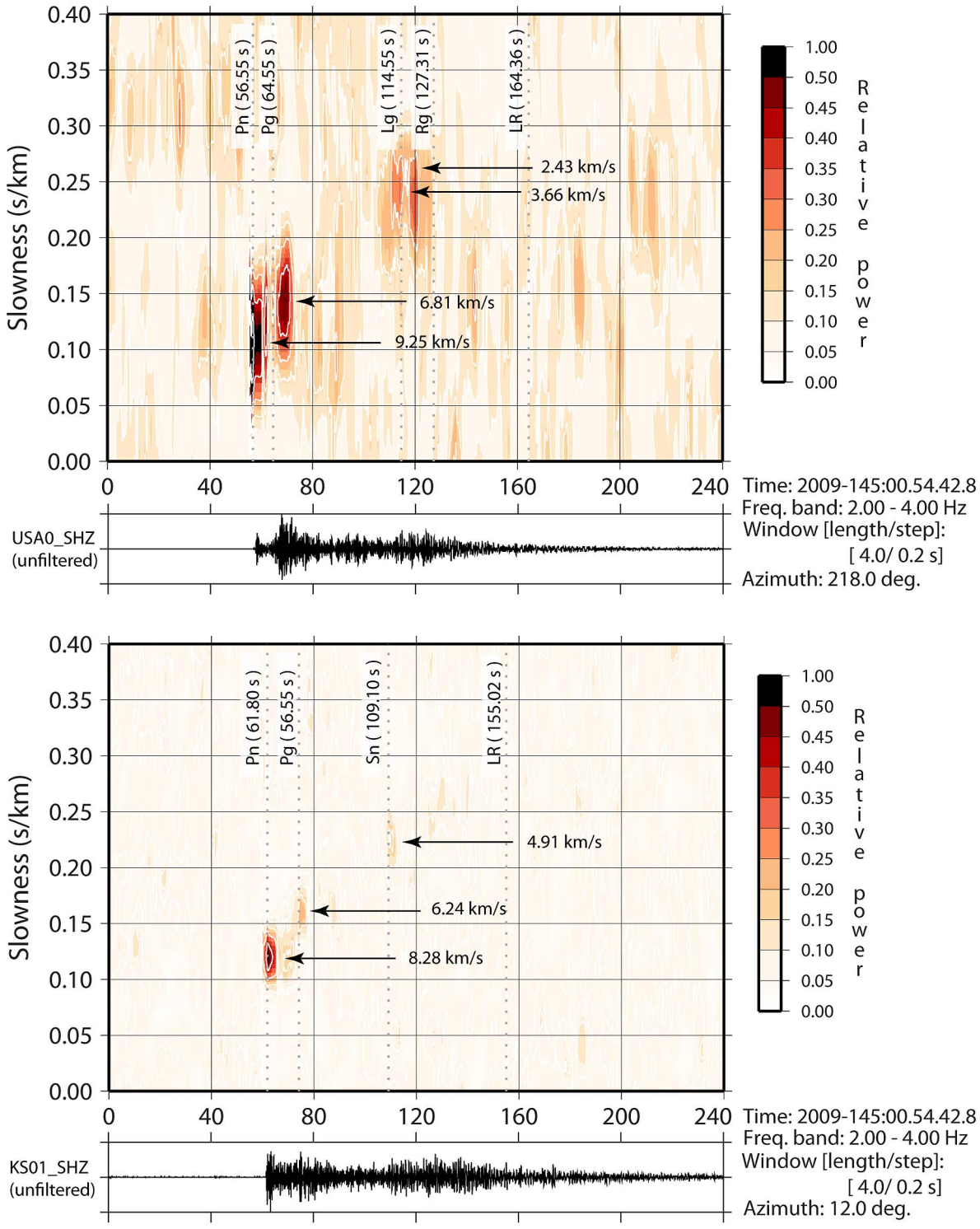

Fig. 2. Vespagrams [17] for the 2009 event signals on the USRK and KSRS arrays. Each panel displays a relative power (the ratio of energy in the beam to the mean energy of the individual traces) where the beam is constructed according to time delays determined by the fixed backazimuth and an apparent velocity $v_{\mathrm{app}} = 1/\mathrm{s\ kms}^{-1}$. A single channel trace is displayed for each array.

space. In practice, it becomes unstable due to the increasing significance of sidelobes in the array response function (ARF) (spatial aliassing) and diminishing waveform coherence. These effects can only be mitigated by augmenting the arrays with additional, more densely spaced, sensors.

The significant maxima of the coherence measures in the USRK and KSRS vespagrams in Fig. 2 confirm that the regional phases from events at the North Korea test site are detectable at these arrays using coherence-based procedures (e.g., [25] and [26]) and that the slowness vectors can be estimated using

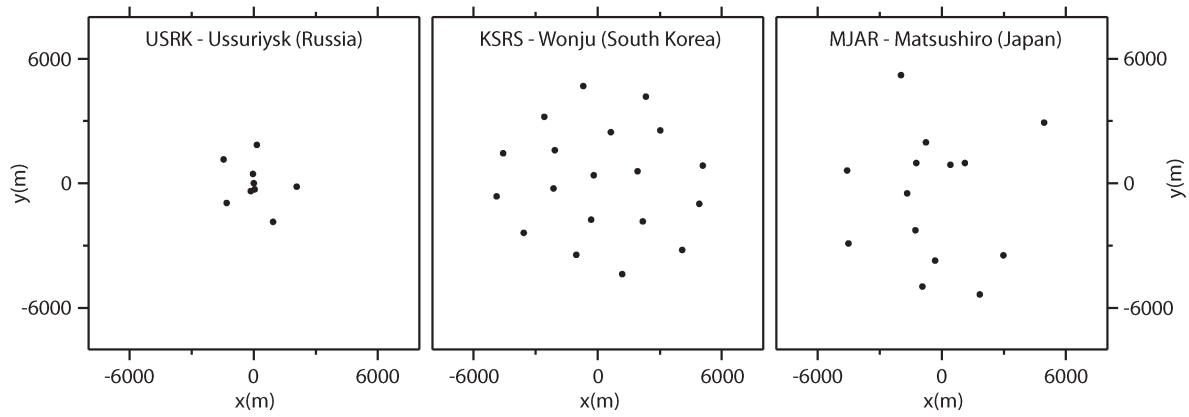

Fig. 3. Geometries of the three closest primary seismic IMS array stations displayed in Fig. 1.

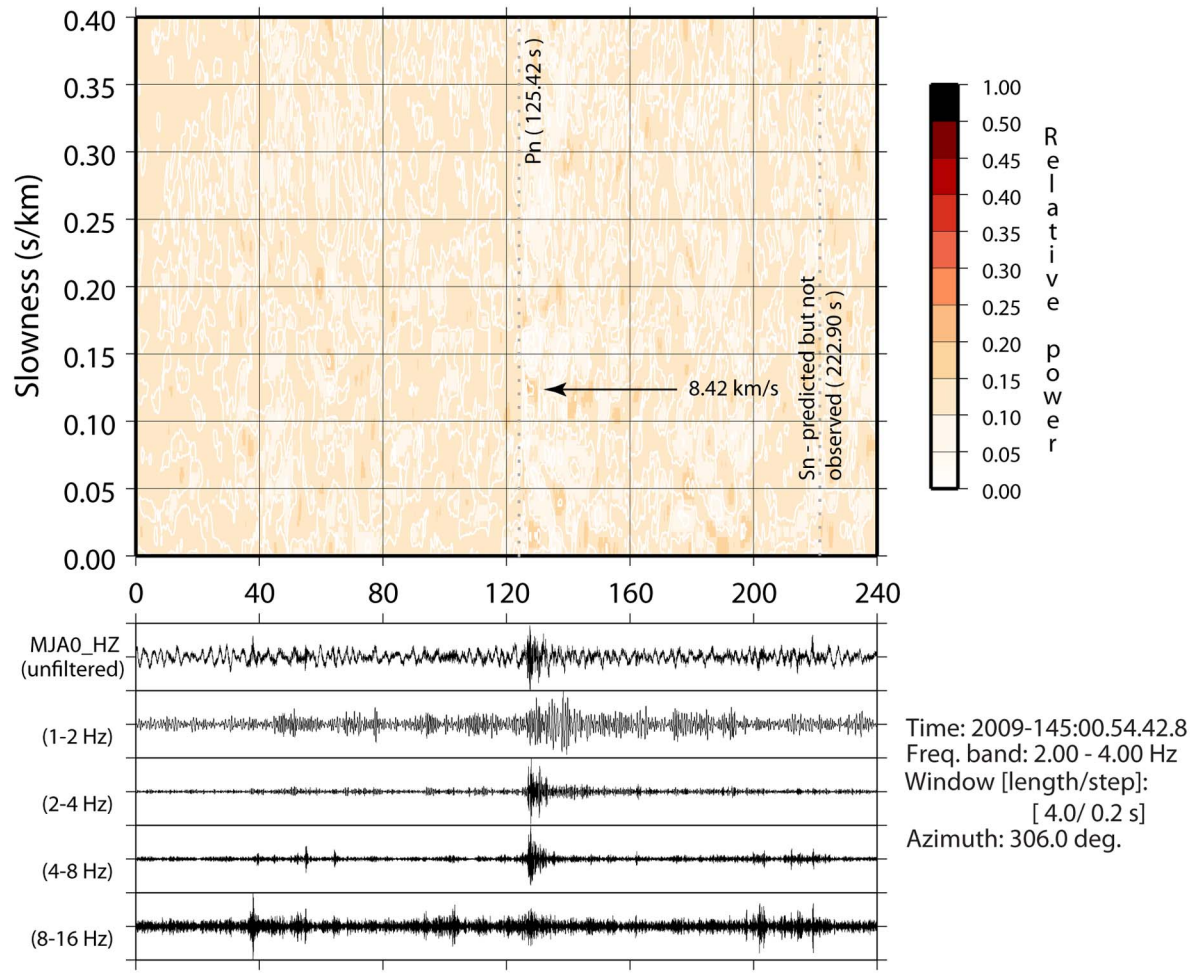

Fig. 4. Vespagram for the 2009 event signal on the MJAR array. The MJA0_HZ channel is displayed both unfiltered and bandpass filtered as indicated.

classical f-k analysis (e.g., [11] and [21]). This is in contrast to the Pn arrival at MJAR (Fig. 4) which, while clearly visible in the high-frequency waveforms, does not result in a significant peak in the vespagram. The waveforms in Fig. 4 and spectra in Fig. 5 suggest that the failure of coherent processing in the 2–4 Hz is not an SNR issue, and the comparable intersite distances and array apertures of KSRS and MJAR (Fig. 3) indicate that the greater local geologic heterogeneity at MJAR is the principal cause of the waveform dissimilarity (cf. [9]). No secondary phases are visible in the waveforms at MJAR, and the clear absence of the Lg phase is to be anticipated from previous studies of regional phase propagation across the Sea of Japan [27]. (See [28] for a discussion of Lg-blockage by sedimentary basins.)

In the absence of waveform semblance at any frequencies with a sufficiently high SNR, we are restricted to incoherent methods for the "blind" detection and estimation of arrivals [10] (subject to the corresponding increase in detection

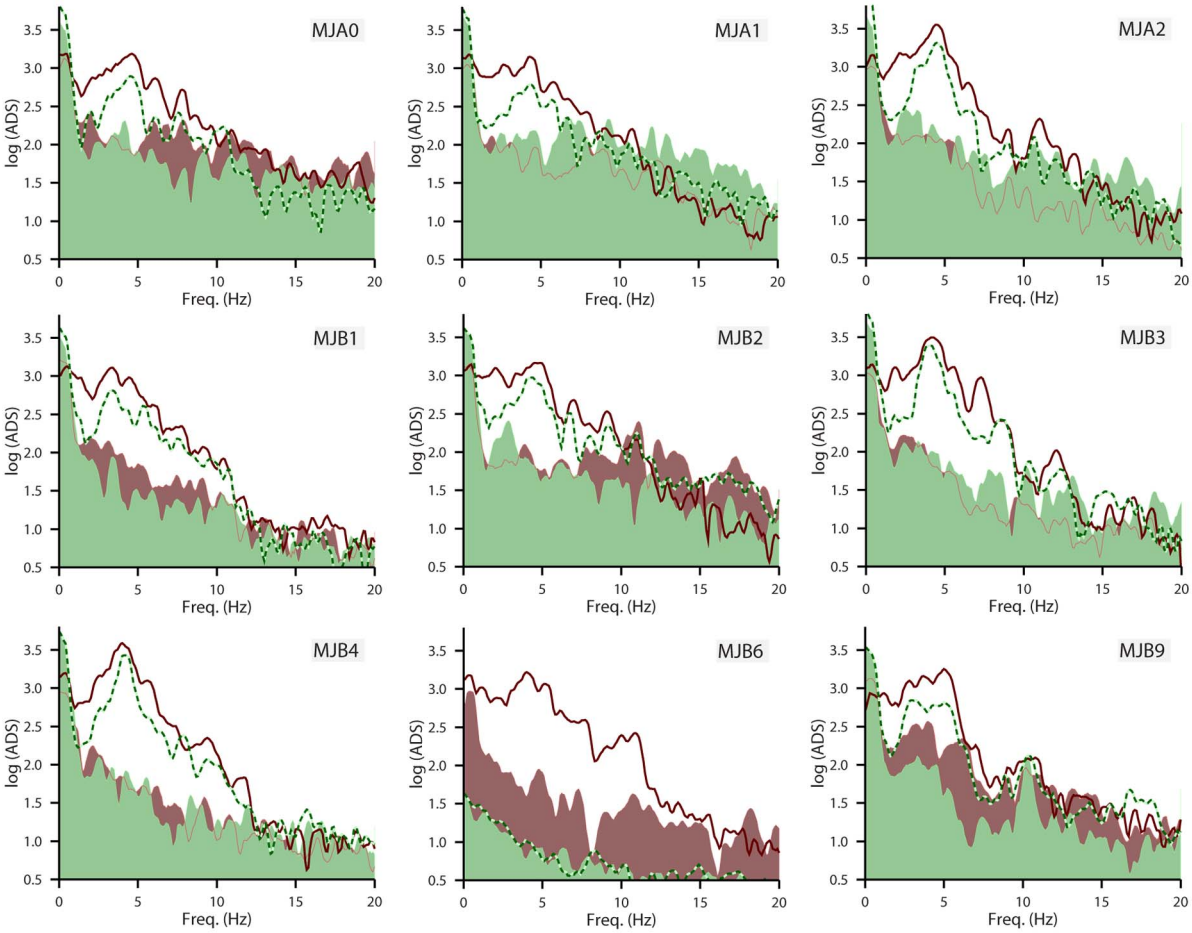

Fig. 5. Spectra from MJAR vertical sensor waveforms as labeled for the 2006 (green) and 2009 (brown) DPRK nuclear tests. All estimates displayed are made from 10.0 s long data segments using the multitaper method [29] (seven tapers). If t_{P} denotes the starting time of the signal data window, at 2006-282:01.37.33.400 and 2009-145:00.56.49.000 for the two events, the noise window begins 13.0 s before t_{P}. The signal spectra are displayed with lines and the noise spectra with solid shapes, although only the outline is displayed when one noise spectrum is obscured by the other. There is evidently a fault with the data in the channel MJB6 at the time of the 2006 test.

threshold and reduction in slowness resolution). In the alternative matched filter or correlation detection procedure, the condition of coherence between sensors is replaced by a condition of similarity between signals from subsequent events. The likeness of the 2006 and 2009 signals at numerous stations globally, together with the resulting relative location estimates [7], [8], indicates that a correlation detector could provide a robust and low-threshold seismic detector over a source region covering many square kilometers. Unlike the continental regional wavetrains displayed in Fig. 2, we have only a very transient signal at MJAR comprising the Pn arrival and a rapidly decaying coda which is close to the background noise level after only 10–15 s. The sensitivity and false alarm rate of a correlation detector depend upon the complexity of the signal (its time-bandwidth product). We therefore seek the widest frequency band possible which is not likely to be subject to an excessive loss of SNR given a significantly smaller event.

The spectra of the Pn arrivals and preceding noise at nine sites of MJAR are displayed in Fig. 5 for both 2006 and 2009 tests. The energy peaks at around 4 Hz for both events, at most sites, although there is significant variation from sensor to sensor with respect to the pattern and frequencies of secondary peaks. The spectral shapes from one event to the next on a single sensor are far more similar than the spectral shapes for the same event on adjacent sensors. This is especially significant for the most closely spaced sites of the array, given that the estimated separation of the two nuclear explosions (between 1.5 and 2.5 km) is slightly larger than the smallest intersensor distances. For the outer elements of the array, this is to be anticipated given that the intersensor spacings are greater than the distance between the sources. The greatest spectral differences between the 2006 and 2009 signals are at the lowest frequencies (1–2 Hz). Based upon the frequency range over which the signal for the 2006 event exceeds the background noise, the 2–8 Hz band was deemed to give a reasonable compromise between maximizing bandwidth and maintaining SNR. While the signal spectra for some sensors clearly exceed the corresponding background noise spectra at frequencies above 8 Hz, this does not apply to all sensors, and the inclusion of the highest frequencies may also make the detector more sensitive to small scale ground motions and reduce the size of the template's geographic footprint. Following a similar consideration of the time-series, bandpass filtered in the 2–8 Hz frequency band, a 10-s long segment was deemed to be optimal.

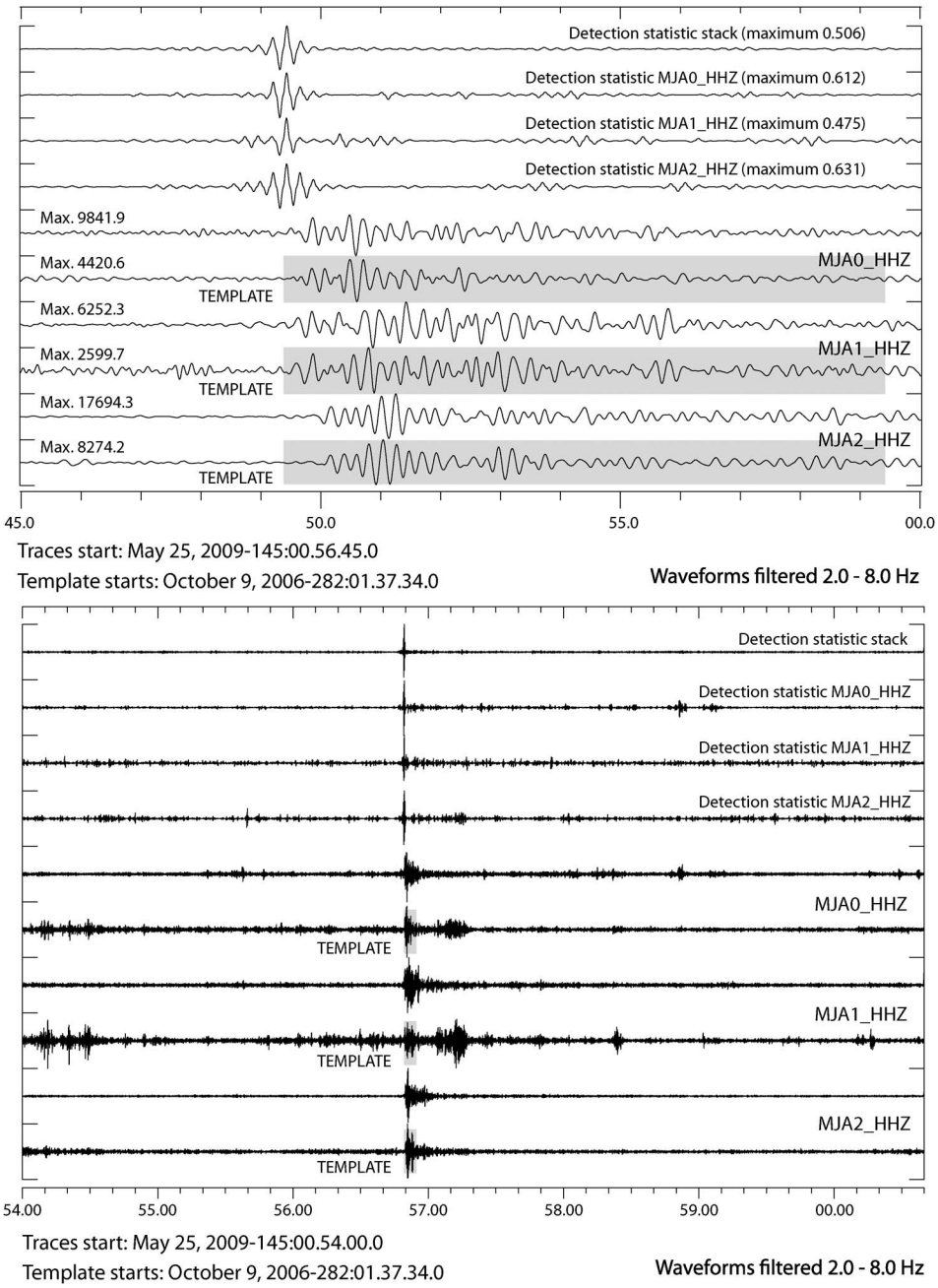

Fig. 6. Waveforms from three channels of the MJAR array from the May 25, 2009, DPRK nuclear test aligned with the corresponding waveforms from the October 9, 2006, event. The corresponding individual channel detection statistic traces are displayed with the array stack. The upper panel is a close-up of the lower panel.

III. Correlation Detector on the MJAR Array for the North Korea Nuclear Test Site

A. Formulation

The vector of N consecutive time samples containing the waveform template recorded on sensor i is denoted $\boldsymbol{x}_i$, where it is understood that the data was scaled *a priori* to give a unit 2-norm, i.e.,

$$\boldsymbol{x}_i.\boldsymbol{x}_i = 1. \tag{1}$$

It is noted that the waveforms are bandpass filtered (in this case between 2 and 8 Hz) prior to cutting the template waveforms. The 10-s long waveform templates for the 2006 signal on three channels of MJAR are displayed in the shaded boxes of Fig. 6.

If $\boldsymbol{y}_i(t)$ denotes the vector of N consecutive time samples starting at time t on sensor i, then

$$C_i(t) = \frac{(\boldsymbol{x}_i.\boldsymbol{y}_i(t))\,\mathrm{abs}\,(\boldsymbol{x}_i.\boldsymbol{y}_i(t))}{(\boldsymbol{y}_i(t).\boldsymbol{y}_i(t))} \tag{2}$$

provides a signal-specific detection statistic for this single sensor indicating the degree of similarity between the unit-norm template vector and the time series beginning at time t. $C_i(t)$ resembles the square of the fully normalized correlation coefficient (avoiding the computational expense of calculating

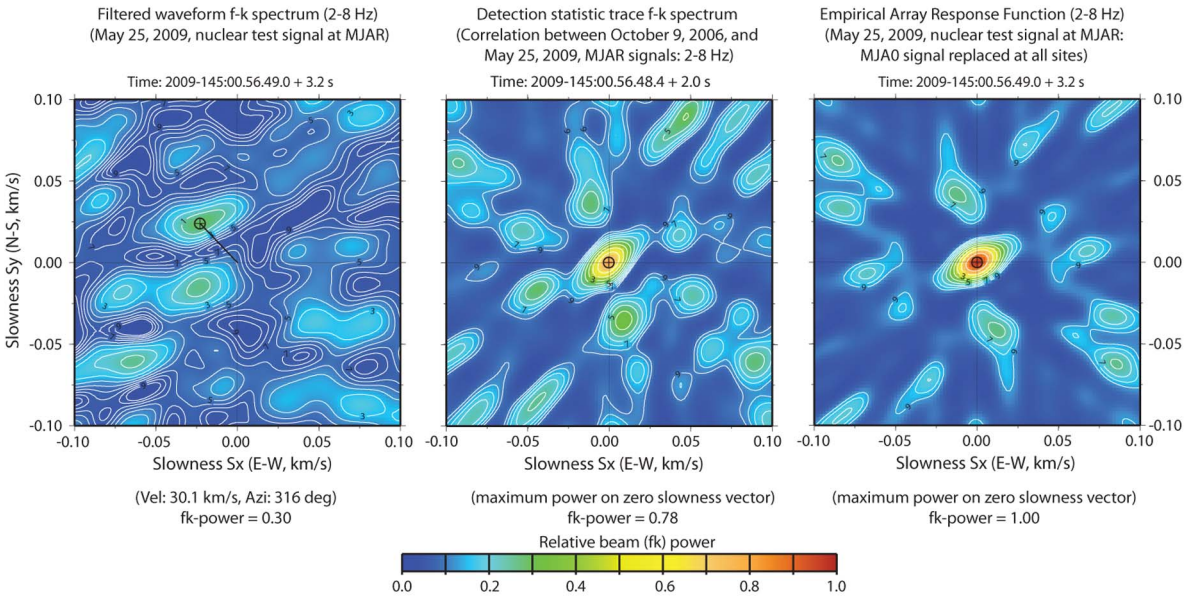

Fig. 7. Frequency-wavenumber spectrum on the MJAR array of (left) a 3.2 s long data window for Pn arrival for the 2009 test, (center) for the single channel detection statistic traces for a 2.0 s window centered at the time of the local maximum (see Fig. 6), and (right) an estimate of the broadband array response function (ARF). The calculations involved in obtaining the f-k spectra in the left and right panels are identical except that, for the ARF, the waveforms at all sites have been replaced with the filtered waveform on the MJA0 sensor. This illustrates how the array would respond to a perfectly coherent wavefront, with the same frequency content as the nuclear test signal, approaching all sensors simultaneously.

the square roots for each sample) but maintains the sign such that the array detection statistic for M sensors

$$C(t) = M^{-1} \sum_{i=1}^{M} C_i(t) \tag{3}$$

results in cancellation in the absence of alignment of features in the individual traces. Most importantly, given a detection on $C(t)$, performing f-k analysis on the individual detection statistic traces [13] allows any detection resulting from coincidental similarity between two wavefronts approaching from slightly different directions to be screened out automatically. This postprocessing step would not be possible had the sign information been lost, and has been demonstrated to filter out the vast majority of false alarms when detecting events from a source of repeating seismicity even when there is significant waveform dissimilarity between subsequent events [30].

For efficiency, all correlations are performed as multiplications in the frequency domain. Correlations for estimating time shifts between transient seismic phases for optimal waveform alignment (e.g., [31]) frequently require subsample precision. The short duration of such signals is problematic for frequency domain methods and, more recently, advanced procedures for waveform alignment [32], [33] use multitaper methods [29] for spectral estimation. In the correlation detectors discussed here, there is no need for subsample precision, and the relatively long length of the time series mean that multiple tapers are not necessary.

Above each of the template waveforms in Fig. 6 is displayed the continuous waveform data at the time of the signal from the 2009 event, aligned according to the maximum value of the array detection statistic, $C(t)$, displayed at the top. The incoming data stream is bandpass filtered in the same frequency band as the waveform template prior to the correlation. The upper panel of Fig. 6 displays a 15-s long section of the waveforms and corresponding detection statistics, confirming the close ripple-for-ripple correspondence between the signals from the two nuclear tests and demonstrating that the maximum value of $C(t)$ is significantly greater than the peaks of the sidelobes. The lower panel displays 7 min of the same functions and demonstrates that the value of $C(t)$ at the time of the maximum is significantly higher than at any other time during this extended section. This builds confidence that the time-bandwidth product of the waveform template provides a signal complexity which is sufficiently high for a low detection threshold to be set with few triggers.

Any detector requires a threshold which must be exceeded in order for a detection to be reported. In this study, we follow an idea similar to that of [34] where triggers are identified as outliers to the distribution of the detection statistic in a given time interval. This provides an absolute threshold that is adjusted dynamically according to the background at a given time. First, the statistic $C(t)$ is evaluated over a window of continuous data, typically of length close to 20 min. Second, the extreme 1% of these values are removed, and the standard deviation of the remaining values calculated. Finally, the ratio between $C(t)$ and this standard deviation is returned and referred to here as the "detection statistic SNR" (DSSNR). If this value exceeds a specified threshold then a preliminary detection is declared and frequency-wavenumber analysis carried on the individual detection statistic traces.

The center panel of Fig. 7 displays the f-k spectrum for the detection statistic traces for the 2009 data stream and the 2006 signal template. As required for the detection to be considered

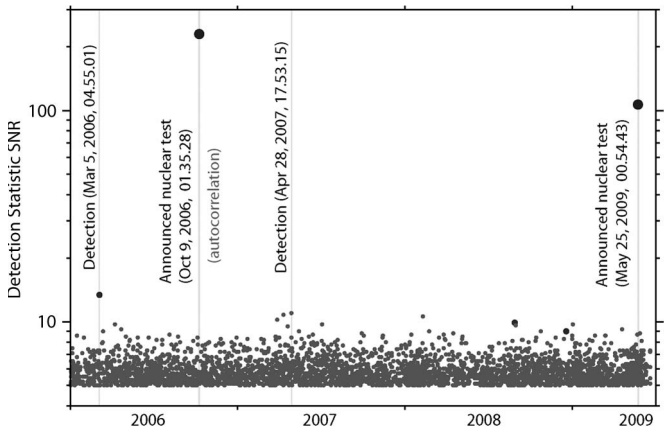

Fig. 8. Detections from the correlator on the MJAR array where the 10-s long signal template begins at a time 2006-282:01.37.32.6. The value denoted "Detection statistic SNR" is described in the text and measures the ratio between the array detection statistic $C(t)$ defined in (3) and the background level of the same quantity. Vertical bars indicate the times of the four highest values obtained in the period January 1, 2006, to June 20, 2009.

further, the maximum value is associated with an almost-zero slowness vector and a high value of the relative beam power (a measure of pattern alignment). For comparison, the left and right hand panels of Fig. 7 display the f-k spectrum for the 2009 MJAR Pn arrival and an estimate of the broadband empirical ARF, respectively. If the arrival was a perfectly coherent plane wavefront, the pattern in the left panel would resemble closely the ARF, only centered on the theoretical slowness vector for the arrival. The site effects at each of the sensors are removed by correlating the two signals, resulting in almost exactly aligned waveforms with a similar frequency content to the original waveforms. This explains the similarity between the a detection statistic f-k spectrum (center panel) and ARF (right hand panel), such that the appropriate criteria for accepting detections based upon the f-k post-processing can be selected simply be examining the ARF.

For each detection made, the detection statistic trace was masked such that no further detections could be declared within 4 s of the local maximum. This avoids multiple declarations within short time windows, which are almost always associated with false alarms.

B. Results for the Period January 1, 2006, to June 20, 2009

Preliminary detections were declared when the DSSNR value exceeded 5.0. Of these, a detection was passed if the amplitude of the slowness vector in the f-k postprocessing did not exceed 0.01 s/km and if the relative power exceeded 0.20. These detections are displayed in Fig. 8 as a function of time. There is almost an order of magnitude factor between the DSSNR corresponding to the detection of the signal from the 2009 test and the next highest value. The distribution of points in the scatter plots indicates that a working threshold of 10.0 would result in a very limited number of detections in the three-year period and that any threshold lower than this would result in far greater numbers, all of which would probably warrant manual analysis. Table II indicates the number of detections reported for different thresholds of this ratio. With an appropriate and

TABLE II
NUMBER OF DETECTIONS OBTAINED BETWEEN JANUARY 1, 2006, AND JUNE 20, 2009, AS A FUNCTION OF THE REQUIRED DETECTION STATISTIC RATIO (DSSNR)

Ratio threshold	Number of detections
14.0	2
13.0	3
12.0	3
11.0	4
10.0	7
9.0	20
8.0	88
7.0	356
6.0	1248
5.0	3632

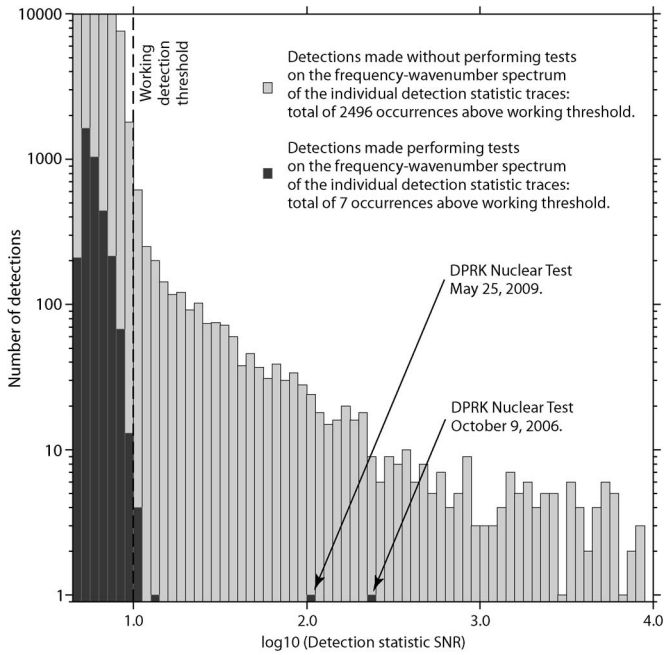

Fig. 9. Histograms of correlation detections with and without f-k postprocessing on the individual channel detection statistic traces. The number of detections in each bin corresponds to the time interval displayed in Fig. 8. 209 detections obtained without the f-k postprocessing exceed the detection statistic SNR for the autocorrelation. All of these detections are the result of faults in the data (e.g., gaps).

conservative detection threshold, the 2009 test could have been detected from the template of the 2006 test with no false alarms. However, for any kind of robust monitoring of a given source region, we need to set as low a threshold as possible to allow for an acceptable degree of waveform dissimilarity.

The first comment on the occurrence of false alarms is to stress the importance of the f-k postprocessing. Fig. 9 indicates, for intervals of the array DSSNR, the number of detections obtained both with and without the automatic screening of detections which fail to meet the requirements of the f-k post-processing algorithm. Without this waveform-alignment test, 2496 as opposed to seven detections would have been registered over a provisional threshold SNR of 10.0 in the test period. This clearly constitutes a dramatic reduction in the human resources necessary to evaluate the detector output.

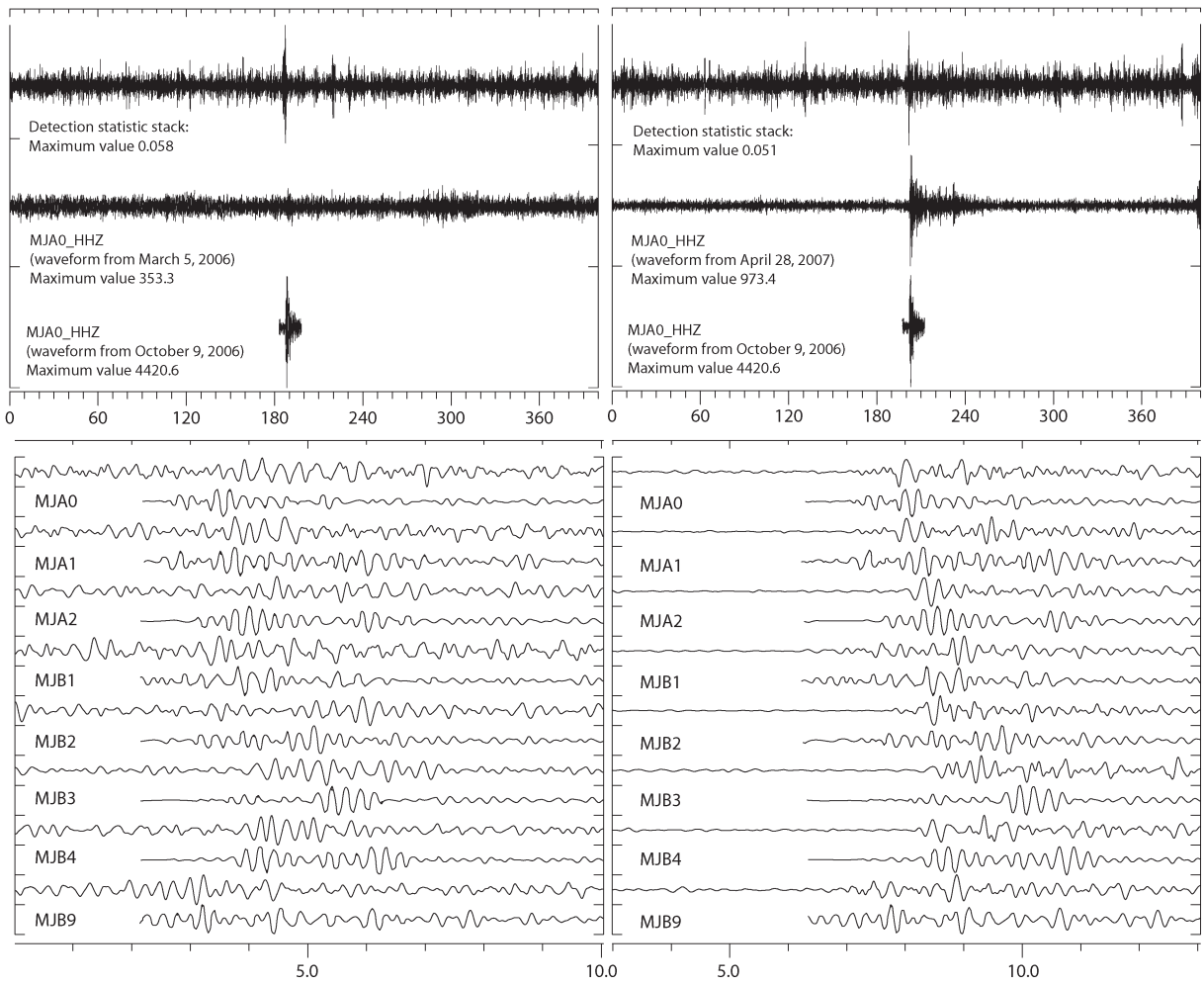

Fig. 10. Waveforms and detection statistic stack traces for the two correlation detections with the highest values of the detection statistic SNR (the announced nuclear tests excluded). In each waveform couplet, the lowermost trace is the template from the 2006 DPRK nuclear test signal.

Many of the detections at the lower SNR end of the spectrum are indeed caused by seismic background noise and wavefronts arriving from somewhat different directions. At the higher SNR end of the spectrum, the detections which are eliminated by the f-k postprocessing are almost exclusively the result of faults in the data: e.g., gaps and spikes. A data discontinuity will frequently either affect one channel only or will affect all channels simultaneously. The multichannel waveform template has encoded an intrinsic time dependence which is only likely to produce aligned correlation coefficient traces if the incoming wavefield encodes the same time dependence. It is of course frequently possible to exclude many such false alarms by other quality control methods. However, the simplicity of the f-k postprocessing method, coupled with its ability to screen a full spectrum of false alarms, makes it both a robust and effective method of online, automatic quality control.

C. Examination of False Alarms

Of the small number of detections which both exceeded the nominal detection threshold and which passed the f-k postprocessing tests, the two detections with highest DSSNR are displayed in Fig. 10. The second of these detections is the easiest to analyze. The waveform template correlates best with a visible signal having an SNR comparable to that of the master event arrival. The bulletin of the International Seismological Center (ISC, http://www.isc.ac.uk/) lists an event with magnitude 2.2, origin time 2007-118:17.54.52.3, epicenter 37.45° N and 136.46° E, and depth 9 km (almost certainly a shallow, offshore earthquake). The ISC location of this event is displayed in relation to the MJAR array in Fig. 11; the backazimuth from MJAR to this event (at 185 km) is almost identical to that for the North Korea test site (at 956 km). The implication of this is that while the source type and location of the events were very different, due to the fact that the resulting wavefront has propagated through the rock close to the array in almost the same direction as the wavefront from the nuclear test, both the correlation and the alignment of waveforms were sufficiently good to result in a detection.

The detection displayed in the left-hand panel of Fig. 10 does not appear to result from a visible signal, and no event is present in the ISC bulletin which could have generated a signal at this time and place. The segment of data which correlates best with the template starting at time 2006-282:01.37.34.0 begins at a time 2006-064:04.57.07.4. Data from the INCN and MDJ stations (in South Korea and China, respectively) were obtained from the IRIS DMC for this time period, and no evidence was observed in these waveforms for an event close to the test site.

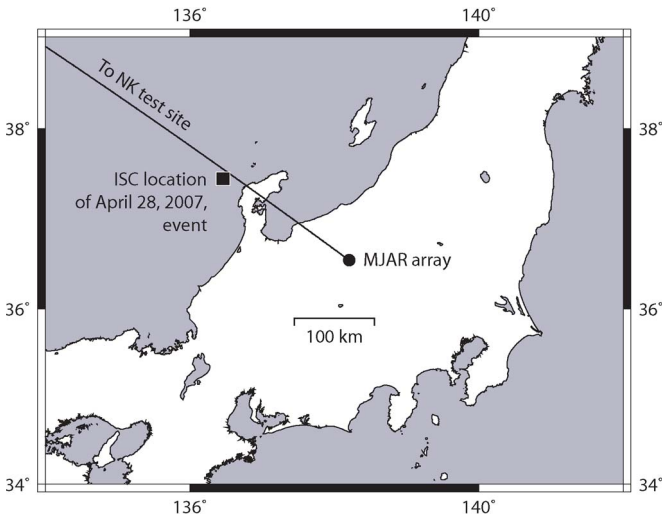

Fig. 11. ISC location of the April 28, 2007, event relative to the MJAR array.

IV. Examining the Detection Threshold

It is of great interest to examine how effective the correlation procedure is at detecting copies of the signals from the two announced nuclear tests, scaled down and submerged into background noise on the MJAR array. The experiment is designed to examine the magnitudes down to which events will be detected reliably using the correlation procedure. No spectral rescaling is applied to the data. We defend a linear scaling of filtered waveforms by referring to a detection study of earthquakes in northern Norway [35] in which a template from a magnitude 3.5 earthquake is used to detect events down to magnitude 0.5 over a distance of over 600 km. It is assumed that the dimensions of the source of the North Korea events are sufficiently limited that the signals generated in the frequency band of interest will not differ significantly as the yield is reduced.

Two different experiments were carried out. In the first, copies of the signal from the 2006 test were scaled down into background noise and, in the second, copies of the signal from the 2009 test were used. In all cases, the waveform template used for the matched filter was the signal from the 2006 test. Both experiments were essentially a repeat of the standard detection run described above, except that for every 20-min long segment of data, a scaling factor between 0.0001 and 1.0 was selected (pseudorandomly), and a copy of the signal of interest was submerged into the data with this scaling. The scaling factor was chosen using the random number algorithm `ran1` provided by [36], with the seed integer picked from the first sample of the top trace of the raw waveform data. This procedure provided a satisfactory distribution of the scaling factors over the three-year interval and was reproducible, allowing data segments containing the scaled signals to be re-examined if necessary without storing the modified waveforms.

The results of this study are displayed in Fig. 12 where the scaling factor applied has been converted to an indication of the inferred event magnitude as shown. There is clearly a large spread in the values of the DSSNR for any given scaling factor. The time period explored extends from January 1, 2006, to June 20, 2009, and—considering that one submerged signal was added to the data every 20 min during this period—we

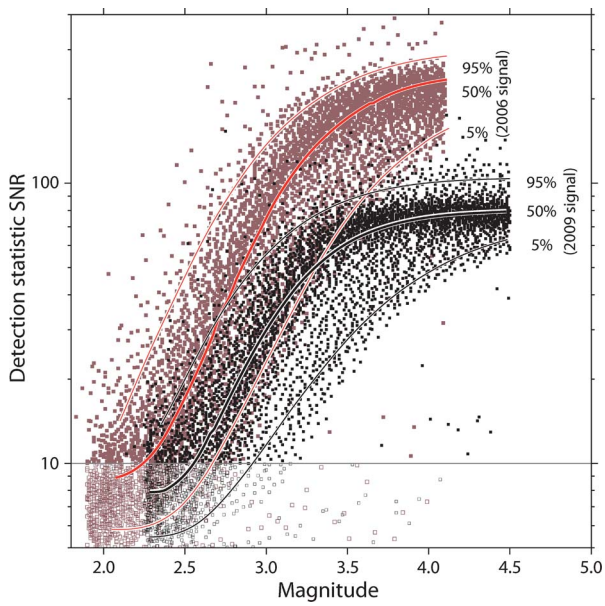

Fig. 12. Detectability using a multichannel correlator on the MJAR array of signals from the 2006 and 2009 explosions, scaled down into different segments of background noise, using the signal from the 2006 explosion as a template. The m_b magnitudes for the 2006 and 2009 events are assumed to be 4.1 and 4.5, respectively, and the magnitude of the simulated events are taken to be $4.1 + \log_{10}(\varepsilon)$ and $4.5 + \log_{10}(\varepsilon)$ where ε is the factor that the explosion signal is scaled by before adding to the background noise at a given time. Only one in 50 of the points used to estimate the detectability curves is plotted on the graph. The detectability curves are based on the points contained in intervals of 0.05 magnitude units.

cover every eventuality of background noise level, including the codas of signals from large earthquakes.

The DSSNR for the scaled-down copies of the 2006 signal decreases almost immediately as the magnitudes of the simulated events decrease. The DSSNR values for the scaled down copies of the 2009 signal start at a lower level than for the 2006 signal (since the signals do have a slightly different form to the detection template) but are not affected greatly by applying a scaling factor between 0.1 and 1.0 (probably due to the large SNR of the 2009 signal). Down to a simulated magnitude of approximately 2.7, 95% of the submerged 2006 signals are still recording DSSNR values above the nominal threshold of 10.0. The same is true for simulated copies of the 2009 event down to magnitudes of around 3.0. 50% of the 2009 signals scaled down to magnitude 2.6 are detected as are 50% of the 2006 signals scaled down to magnitude 2.3.

V. Conclusion

We have demonstrated that performing multichannel cross-correlation on the MJAR array in Japan, using a signal template taken from the October 9, 2006, North Korea nuclear test, is able to detect the signals from the May 25, 2009, North Korea test with a very low false alarm rate. Crucial to the low false alarm rate in this study is the performing of f-k analysis on the individual sensor detection statistic traces which eliminates false alarms both due to unrelated seismic signals and problems in the data.

A scaling study, whereby signals from both 2006 and 2009 tests are scaled down and submerged into the background

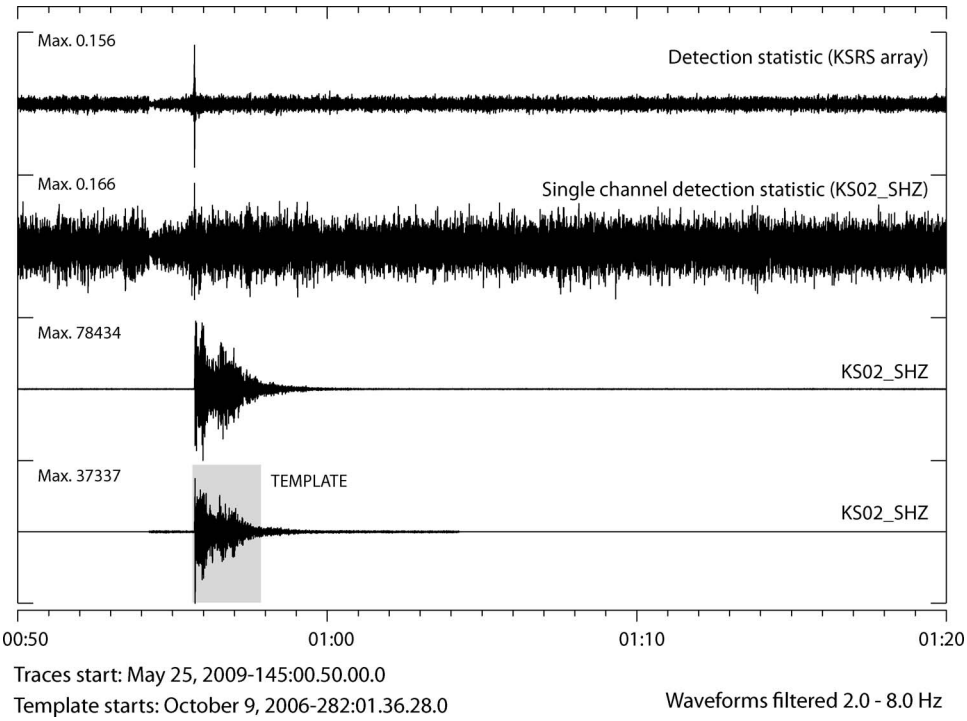

Fig. 13. Correlation of a 120-s long template from the October 9, 2006, DPRK test with a 30-min long data segment on May 25, 2009, on the KSRS array in the Republic of Korea. Only the channel KS02_SHZ is shown although the array detection statistic trace is constructed using all 19 short period vertical channels of the array. The template waveform is aligned with the 2009 signal according to the time of the maximum of the detection statistic trace. The importance of stacking the single channel detection statistic channels over the array is evident. The DSSNR in the above plot is 65.0, in comparison with 106.7 for the calculation on the MJAR array.

noise, suggests that, at a detection threshold which results in a negligible number of triggers, events down to magnitude 3.0 at the site of the 2009 test are detected by the correlation procedure in 95% of cases.

The single array monitoring case is of special interest since it may provide a degree of redundancy in the global network and mitigate the effects of station outages. Existing association procedures for regional and global networks, e.g., [37], may be affected greatly by the absence of data from one or more stations. The correlation detector [13] combines the detection, identification, and location in a single operation and so can be run independently for many array stations in parallel. Correlation detections obtained from independent processes on different arrays, consistent with a single source location and event origin time, will reduce further the likelihood of false alarms. For example, the false alarm resulting from the regional earthquake in Fig. 11 is very unlikely to have produced a detection on any other array than MJAR.

Since the IMS that recorded the 2009 explosion is far more complete than that which recorded the 2006 explosion, we are in a far better position to apply the same procedures for the detection of any subsequent events. For many stations, there are now two signal templates and the applicable geographical footprint should now cover an increased region surrounding the test site. MJAR was selected for the current study firstly because it was the only certified primary IMS array within regional distances of the North Korea test site at the time of the 2006 test and, second, because conventional array and network processing had failed to utilize the signals on this station for detection or the automatic location estimate.

There are many IMS arrays at teleseismic distances that recorded the 2006 test (e.g., [8]) and the procedure described here could be applied to each one of these. The sensitivity and false alarm rates associated with correlators at each station need to be investigated on a case-by-case basis. The performance at each station is likely to be a function of signal complexity (e.g., time-bandwidth product), coherence between sensors (waveform dissimilarity may actually improve the performance of a correlation detector since the signature fingerprint of the source region is so different for each sensor, providing more degrees of freedom in the waveform template), SNR, and the presence of additional sources of seismicity along the test site to receiver path. The correlation using KSRS is displayed in Fig. 13, with the 2006 signal taken from the then uncertified station. There is less similarity between the 2006 and 2009 signals on KSRS than on MJAR and the maximum value of the single channel detection statistic is barely above the background level. However, the stacking operation over the full 19 site array results in a network detection statistic with a significant local maximum. The longer duration continental regional wavetrain provides a template which is more difficult to match by coincidence, reducing the background level of the DS, and the performance of the long-term correlation detector is comparable to that of MJAR.

Subspace detectors [38]–[40] are a generalization of correlation detectors that, instead of a single multichannel waveform template, utilize an ensemble of template waveforms and allow greater signal variability at the expense of increasing the false alarm rate. Another form of a pattern-specific detector is provided by empirical matched field processing [41] which

exploits a narrow-frequency band representation of the signal over a network of sensors. This procedure is sensitive to the spatial structure of the wavefield and less sensitive to the temporal structure, making it ideal for the classification of repeating seismic sources which display significant variation in the source-time function. However, given the high similarity between the waveforms from the two confirmed nuclear tests at this site, it is to be expected that correlation detectors (rank-1 subspace detectors) provide the optimal detector for this limited source region. The most significant improvements to the sensitivity and robustness of this procedure are likely to come from network processing of multiple correlation detectors regionally and globally.

This paper has considered only seismic monitoring, one of the four technologies comprising the CTBT verification regime. There is increasing interest in satellite sensing for monitoring damage and surface changes due to both earthquakes (e.g., [42]) and underground nuclear tests (e.g., [43] and [44]). The availability of high-quality commercial satellite imagery has improved dramatically since the inception of the Treaty and, while satellite imaging is not a CTBT verification technology, it is likely to become an increasingly significant part of nuclear explosion monitoring carried out by nation states. Images before and after the 2006 test identified changes indicative of infrastructure development which corroborated the seismic event location estimates [45], and, following the 2009 test, satellite imagery was used to assess the relative event location estimates ([7], [46]). In the future, we may expect an increased synergy between precision seismology and satellite remote sensing with absolute and relative seismic location estimates limiting search regions for analysis of satellite imagery, and satellite-inferred topographic constraints improving our understanding of source-related waveform characteristics and inter-event waveform similarity.

ACKNOWLEDGMENT

IMS waveform data were acquired via the IDC in Vienna. Data from the MDJ and INCN stations were obtained via the IRIS Data Management Center and are made available via the IC and IU networks, respectively. All maps were generated using GMT software [47].We thank Dr. Heon Cheol Chi of the Korea Institute of Geoscience and Mineral Resources for providing the segment of KSRS data for the 2006 test.

REFERENCES

[1] O. Dahlman, S. Mykkeltveit, and H. Haak, *Nuclear Test Ban: Converting Political Visions to Reality*. Dordrecht, The Netherlands: Springer Media B.V., 2009.

[2] T. Kværna, F. Ringdal, and U. Baadshaug, "North Korea's nuclear test: The capability for seismic monitoring of the North Korean test site," *Seismol. Res. Lett.*, vol. 78, no. 5, pp. 487–497, Sep. 2007.

[3] P. G. Richards and W.-Y. Kim, "Seismic signature," *Nat. Phys.*, vol. 3, no. 1, pp. 4–6, Jan. 2007.

[4] W.-Y. Kim and P. G. Richards, "North Korean nuclear test: Seismic discrimination at low yield," *EOS Trans. AGU*, vol. 88, no. 14, pp. 158–161, Apr. 2007.

[5] F. Waldhauser and W. L. Ellsworth, "A double-difference earthquake location algorithm: Method and application to the Northern Hayward Fault, California," *Bull. Seismol. Soc. Amer.*, vol. 90, no. 6, pp. 1353–1368, Dec. 2000.

[6] P. G. Richards, F. Waldhauser, D. Schaff, and W.-Y. Kim, "The applicability of modern methods of earthquake location," *Pure Appl. Geophys.*, vol. 163, no. 2/3, pp. 351–372, Mar. 2006.

[7] L. Wen and H. Long, "High-precision location of North Korea's 2009 nuclear test," *Seismol. Res. Lett.*, vol. 81, no. 1, pp. 26–29, Jan. 2010.

[8] N. D. Selby, "Relative locations of the October 2006 and May 2009 DPRK announced nuclear tests using International Monitoring System seismometer arrays," *Bull. Seismol. Soc. Amer.*, vol. 100, no. 4, pp. 1779–1784, Aug. 2010.

[9] M. Kato, I. Nakanishi, and H. Takayama, "Variation of teleseismic short-period waveforms at Matsuishiro Seismic Array System," *Earth, Planets, Space*, vol. 57, no. 7, pp. 563–570, 2005.

[10] S. J. Gibbons, F. Ringdal, and T. Kværna, "Detection and characterization of seismic phases using continuous spectral estimation on incoherent and partially coherent arrays," *Geophys. J. Int.*, vol. 172, no. 1, pp. 405–421, Jan. 2008.

[11] J. Capon, "High-resolution frequency-wavenumber spectrum analysis," *Proc. IEEE*, vol. 57, no. 8, pp. 1408–1418, Aug. 1969.

[12] W. W. Shen, "A constrained minimum power adaptive beamformer with time-varying adaptation rate," *Geophysics*, vol. 44, no. 6, pp. 1088–1096, Jun. 1979. [Online]. Available: http://dx.doi.org/10.1190/1.1440997

[13] S. J. Gibbons and F. Ringdal, "The detection of low magnitude seismic events using array-based waveform correlation," *Geophys. J. Int.*, vol. 165, no. 1, pp. 149–166, Apr. 2006.

[14] T.-K. Hong, C.-E. Baag, H. Choi, and D.-H. Sheen, "Regional seismic observations of the 9 October 2006 underground nuclear explosion in North Korea and the influence of crustal structure on regional phases," *J. Geophys. Res.*, vol. 113, p. B03 305, 2008. doi:DOI:10.1029/2007JB004950.

[15] T. Kværna, F. Ringdal, and U. Baadshaug, "Detection capability of IMS primary and auxiliary seismic stations," NORSAR, Kjeller, Norway, NORSAR Scientific Report: Semiannual Technical Summary No. 2 - 2009, Aug. 2009.

[16] T. Kværna, F. Ringdal, and J. Given, "Application of detection probabilities in the IDC global phase association process," in *Proc. Monit. Res. Rev.*, Tucson, AZ, Sep. 13–15, 2011, pp. 302–311.

[17] D. Davies, D. J. Kelly, and J. R. Filson, "The VESPA process for the analysis of seismic signals," *Nature*, vol. 232, pp. 8–13, 1971.

[18] S. Rost and C. Thomas, "Array seismology: Methods and applications," *Rev. Geophys.*, vol. 40, no. 3, p. 1008, Dec. 2002. doi:DOI:10.1029/2000RG000100.

[19] J. Schweitzer, J. Fyen, S. Mykkeltveit, and T. Kværna, "Chapter 9: Seismic arrays," in *IASPEI New Manual of Seismological Observatory Practice*, P. Bormann, Ed. Potsdam, Germany: GeoForschungsZentrum, 2002, p. 52.

[20] D. A. Storchak, J. Schweitzer, and P. Bormann, "The IASPEI standard seismic phase list," *Seismol. Res. Lett.*, vol. 74, no. 6, pp. 761–772, Nov./Dec. 2003.

[21] B. L. N. Kennett, *The Seismic Wavefield. Volume II: Interpretation of Seismograms on Regional and Global Scales*. Cambridge, U.K.: Cambridge Univ. Press, 2002.

[22] T. Kværna and F. Ringdal, "Integrated array and three-component processing using a seismic microarray," *Bull. Seismol. Soc. Amer.*, vol. 82, no. 2, pp. 870–882, Apr. 1992.

[23] H. Bungum and E. S. Husebye, "Errors in time delay measurements," *Pure Appl. Geophys.*, vol. 91, no. 1, pp. 56–70, Dec. 1971.

[24] F. Ringdal and E. S. Husebye, "Application of arrays in the detection, location, and identification of seismic events," *Bull. Seismol. Soc. Amer.*, vol. 72, no. 6B, pp. S201–S224, Dec. 1982.

[25] Y. Cansi, "An automatic seismic event processing for detection and location: The P.M.C.C. method," *Geophys. Res. Lett.*, vol. 22, no. 9, pp. 1021–1024, 1995.

[26] N. D. Selby, "Application of a generalized F detector at a seismometer array," *Bull. Seismol. Soc. Amer.*, vol. 98, no. 5, pp. 2469–2481, Oct. 2008.

[27] T. Furumura and B. L. N. Kennett, "Variations in regional phase propagation in the area around Japan," *Bull. Seismol. Soc. Amer.*, vol. 91, no. 4, pp. 667–682, Aug. 2001.

[28] D. R. Baumgardt, "Sedimentary basins and the blockage of Lg wave propagation in the continents," *Pure Appl. Geophys.*, vol. 158, no. 7, pp. 1207–1250, Jul. 2001.

[29] D. J. Thomson, "Spectrum estimation and harmonic analysis," *Proc. IEEE*, vol. 70, no. 9, pp. 1055–1096, Sep. 1982.

[30] S. J. Gibbons and F. Ringdal, "Detection and analysis of near-surface explosions on the Kola Peninsula," *Pure Appl. Geophys.*, vol. 167, no. 4/5, pp. 413–436, May 2010.

[31] M. Simaan, "A frequency-domain method for time-shift estimation and alignment of seismic signals," *IEEE Trans. Geosci. Remote Sens.*, vol. GRS-23, no. 2, pp. 132–138, Mar. 1985.
[32] R. C. Aster and C. A. Rowe, *Automatic Phase Pick Refinement and Similar Event Association in Large Seismic Data Sets*. Amsterdam, The Netherlands: Kluwer, 2000, pp. 231–263.
[33] C. A. Rowe, R. C. Aster, B. Borchers, and C. J. Young, "An automatic, adaptive algorithm for refining phase picks in large seismic data sets," *Bull. Seismol. Soc. Amer.*, vol. 92, no. 5, pp. 1660–1674, Jun. 2002.
[34] D. P. Shelly, G. C. Beroza, and S. Ide, "Non-volcanic tremor and low-frequency earthquake swarms," *Nature*, vol. 446, no. 7133, pp. 305–307, Mar. 2007.
[35] S. J. Gibbons, M. Bøttger-Sørensen, D. B. Harris, and F. Ringdal, "The detection and location of low magnitude earthquakes in northern Norway using multi-channel waveform correlation at regional distances," *Phys. Earth Planet. Interiors*, vol. 160, no. 3/4, pp. 285–309, Mar. 2007.
[36] W. H. Press, B. P. Flannery, S. A. Teukolsky, and W. T. Vetterling, *Numerical Recipes in C: The Art of Scientific Computing*, 2nd ed. Cambridge, U.K.: Cambridge Univ. Press, Oct. 1992.
[37] F. Ringdal and T. Kværna, "A multi-channel processing approach to real time network detection, phase association, and threshold monitoring," *Bull. Seismol. Soc. Amer.*, vol. 79, no. 6, pp. 1927–1940, Dec. 1989.
[38] D. B. Harris, "Subspace detectors: Theory," Lawrence Livermore Nat. Lab., Livermore, CA, Tech. Rep. UCRL-TR-222758, Jul. 2006.
[39] D. B. Harris and T. Paik, "Subspace detectors: Efficient implementation," Lawrence Livermore Nat. Lab., Livermore, CA, Tech. Rep. UCRL-TR-223177, Jul. 2006.
[40] M. Maceira, C. A. Rowe, G. Beroza, and D. Anderson, "Identification of low-frequency earthquakes in non-volcanic tremor using the subspace detector method," *Geophys. Res. Lett.*, vol. 37, no. 6, p. L06 303, 2010.
[41] D. B. Harris and T. Kvaerna, "Superresolution with seismic arrays using empirical matched field processing," *Geophys. J. Int.*, vol. 182, no. 3, pp. 1455–1477, Sep. 2010.
[42] M. Chini, N. Pierdicca, and W. J. Emery, "Exploiting SAR and VHR optical images to quantify damage caused by the 2003 Bam earthquake," *IEEE Trans. Geosci. Remote Sens.*, vol. 47, no. 1, pp. 145–152, Jan. 2009.
[43] M. D. Fisk, "Accurate locations of nuclear explosions at the lop nor test site using alignment of seismograms and IKONOS satellite imagery," *Bull. Seismol. Soc. Amer.*, vol. 92, no. 8, pp. 2911–2925, Dec. 2002. [Online]. Available: http://dx.doi.org/10.1785/0120010268
[44] P. Vincent, S. Larsen, D. Galloway, R. J. Laczniak, W. R. Walter, W. Foxall, and J. J. Zucca, "New signatures of underground nuclear tests revealed by satellite radar interferometry," *Geophys. Res. Lett.*, vol. 30, no. 22, pp. 2141, Nov. 2003. [Online]. Available: http://dx.doi.org/10.1029/2003GL018179
[45] J. Schlittenhardt, M. Canty, and I. Grünberg, "Satellite earth observations support CTBT monitoring: A case study of the nuclear test in North Korea of Oct. 9, 2006 and comparison with seismic results," *Pure Appl. Geophys.*, vol. 167, no. 4, pp. 601–618, May 2010.
[46] J. R. Murphy, B. C. Kohl, J. L. Stevens, T. J. Bennett, and H. G. Israelsson, "Exploitation of the IMS and other data for a comprehensive, advanced analysis of the North Korean nuclear tests," in *Proc. Monit. Res. Rev.: Ground-Based Nucl. Explosion Monit. Technol.*, 2010, pp. 456–465, Report LA-UR-10-05578.
[47] P. Wessel and W. H. F. Smith, "New version of the generic mapping tools released," *EOS Trans. AGU*, vol. 76, no. 33, p. 329, 1995.

Steven J. Gibbons (M'09) received the Ph.D. degree from the School of Computer Studies, University of Leeds, Leeds, U.K., in 1999 and continued studies of numerical simulations in magnetohydrodynamics at the Universities of Exeter and Leeds.

Since March 2002, he has been a Research Geophysicist in the group for Seismology and CTBT Verification at NORSAR. His primary research interests include the use of full-waveform methods for signal detection and identification in verification seismology, optimizing array processing for improved detection and estimation capability, and characterization of the seismo-acoustic wavefield.

Frode Ringdal received the Dr. Philos. degree from the University of Oslo, Oslo, Norway, in 1977 and has more than 40 years of research experience in a wide range of geophysical and data processing-related applications.

Among his primary accomplishments are development of maximum-likelihood magnitudes for estimating the size of seismic events, real-time seismic array detection processing techniques, accurate methods for explosion yield estimation, and innovative methods for seismic network phase association and threshold monitoring. He is currently a Senior Science Advisor at NORSAR.